

NUMERICAL INVESTIGATION ON DYNAMIC RADAR CROSS SECTION OF NAVAL SHIP CONSIDERING OCEAN WAVE-INDUCED MOTION

Kookhyun Kim¹, Jin-Hyeong Kim², Yun-Hwan Kim³, and Dae-Seung Cho^{4, *}

¹Department of Naval Architecture, Tongmyong University, Korea

²Technical Research Institute, Createch Co., Ltd., Korea

³Hyundai Maritime Research Institute, Hyundai Heavy Industries Co., Ltd., Korea

⁴Department of Naval Architecture and Ocean Engineering, Pusan National University, Korea

Abstract—In design phase of naval ships, the effectiveness of RCS reduction means such as shaping, shielding and applying radar absorbing materials is assessed quantitatively via several times of numerical analyses. During the process, in general, the numerical analyses have been carried out only for the static case not considering ship motions in actual ocean environments in spite that ocean waves induce the ship motion of the object naval ship and distort RCS measures. In this study, the dynamic RCS characteristics of the naval ship considering the ocean wave-induced motion have been numerically investigated. For this purpose, a dynamic RCS analysis procedure so called “quasi-static approach” has been adopted for considering the time varying ship motion. The results for two types of naval ships, a stealthy and a non-stealthy ship, show that the RCS of the object naval ships could be reduced or increased in mean value by the ship motion due to the ocean wave, compared to the static RCS value, and also the measures are considerably affected by the various parameters, type of object ship, significant wave height and incident angle of ocean wave, and incident angle of radar wave.

Received 12 October 2012, Accepted 5 November 2012, Scheduled 8 November 2012

* Corresponding author: Dae-Seung Cho (daecho@pusan.ac.kr).

1. INTRODUCTION

The radar cross section (RCS) measure of a naval ship is one of the important design features when considering the survivability in hostile environments. Therefore, various techniques, such as shaping, shielding and applying radar absorbing materials, are applied to RCS reduction of the object naval ship.

In design phase, the effectiveness of the RCS reduction means mentioned above is assessed quantitatively via several times of numerical analyses. In general, most numerical analyses are carried out only for the static case not considering the ship motion. In the actual ocean environment, however, the ocean wave should induce the ship motion and distort the RCS [1]. In practice, the impact of the ship motion is calibrated, based on the real-timely measured ship motion data, in the sea trial after completing shipbuilding [2]. And also the dynamic RCS feature extraction is a crucial factor when developing radar signal processing algorithms. Therefore, an efficient numerical analysis algorithm should be required.

Ojeda et al. have experimentally investigated the dynamic RCS by analyzing the Doppler effects by roll motions, based on the test results of a real ship [3]. And Jamil and Burkholder have carried out the study on the dynamic RCS changes due to the ship motion based on numerical simulations with a 2-dimensional generalized forward-backward (GFB) method [4]. This study is meaningful in a point of view that the first quantitative assessment would be tried, while the study has been restricted to 2-dimensional problems. And also the study has assumed that roll angle would be the same as an inclination of ocean wave, so that could not reflect the actual ship motion characteristics. On the other hand, Kim et al. have suggested a quasi-static approach reflecting the ship motion itself, in the dynamic RCS calculation of naval ships [5].

In this study, the dynamic RCS characteristics of naval ships considering ocean wave-induced motion are numerically investigated using the quasi-static approach. For this purpose, two types of naval ships are selected as the object models. One is a stealthy naval ship applying the shaping techniques such as inclining hull and shielding outdoor equipment for RCS reduction, while the other is a conventional (non-stealthy) naval ship applying no RCS reduction technique.

2. DYNAMIC RCS ANALYSIS

A quasi-static approach is introduced to simulate the dynamic RCS values of naval ship as mentioned above. The approach assumes that

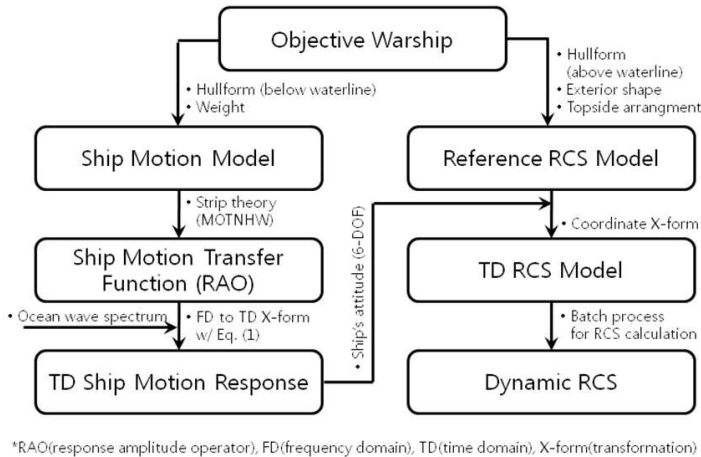


Figure 1. Dynamic radar cross section analysis procedure.

the ship motion would be temporally stopped when radio wave arrives and is applicable to the problem that the propagation speed of the radio wave is much faster than that of ship motion [6].

2.1. Procedure

Figure 1 represents the dynamic RCS analysis procedure in this study. Firstly, the transfer functions of the ship motion, related to response amplitude operators (RAO) [7], are calculated by using a strip theory [8], where the numerical model is generated for the ship motion calculation by referring to the data of hull form under the waterline and the weight data. The time domain ship motion responses could be obtained with the transfer functions calculated and the standard ocean wave spectrum pre-defined.

Meanwhile, a reference RCS model is built by referring to the data of the hull form above waterline, the exterior shape and the topside arrangement of the object naval ship, considering a still water condition (no ship motion). Next, a batch of numerical models are automatically generated with the reference RCS model and the attitude data of each time step by using a converting program separately implemented. Finally, a series of RCS calculations are carried out for all models successively based on a high frequency RCS analysis theory.

2.2. Time Domain Ship Motion Response Calculation

Considering a six-degree-of-freedom (6-DOF) linear system in the Cartesian coordinates defined as Fig. 2, the time domain ship motion

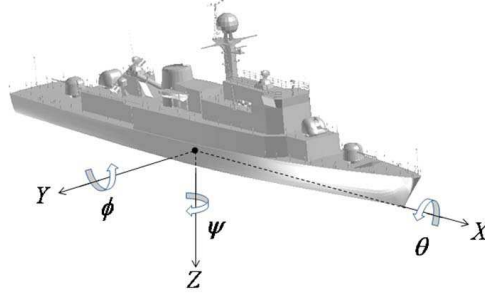


Figure 2. Cartesian coordinates of 6 DOF ship motion.

responses of i -th degree of freedom can be calculated by using the Equation (1) [10].

$$\eta_i(t) = \sum_{k=1}^K \{|H_i(\omega_{e,k})| \cdot \bar{\zeta}_k \cdot \cos[\omega_{e,k}t + \gamma_k + \angle H_i(\omega_{e,k})]\} \quad (1)$$

where $\eta_1 = X$ (surge), $\eta_2 = Y$ (sway), $\eta_3 = Z$ (heave), $\eta_4 = \theta$ (roll), $\eta_5 = \phi$ (pitch), $\eta_6 = \psi$ (yaw) and t is the time. γ_k is the random phase of k -th frequency component. $H_i(\omega_{e,k})$ is the frequency-domain transfer function of i -th degree of freedom and is defined by the following equation:

$$H_i(\omega_{e,k}) = |H_i(\omega_{e,k})| \exp\{\angle H_i(\omega_{e,k})\} \quad (2)$$

where $\omega_{e,k}$ is the encounter frequency of ship against the ocean wave and calculated by the following equation:

$$\omega_{e,k} = |\omega_k \{1 - (V/g) \cos \mu\}| \quad (3)$$

where ω_k is the angular frequency of k -th ocean wave. V is the ship speed and g is the acceleration of gravity. μ is the ocean wave incident angle ($\mu = 0$ degree for heading sea, $\mu = 180$ degree for following sea). $\bar{\zeta}_k$ is the ocean wave amplitude of k -th frequency component obtained by the following equation

$$\bar{\zeta}_k = \sqrt{2 \int_{\omega_k - \Delta\omega_k/2}^{\omega_k + \Delta\omega_k/2} S(\omega) d\omega} \quad (4)$$

where $\Delta\omega_k$ is the angular frequency differential of k -th ocean wave. $S(\omega_k)$ is the ocean wave spectral density function and ω is the ocean wave angular frequency.

2.3. RCS Calculation

In order to calculate the RCS of the numerical model generated in each time step, a combining method of physical optics and geometrical

optics [9, 11] is adopted. The method applies a physical optics for the last reflection point and a geometric optics for the other reflection points, and also is useful for explanation of the polarizations occurred by the single or multiple reflections on dielectrically lossy surfaces as well as perfectly electric conducting (PEC) surfaces.

The radar cross section matrix $[\sigma]$ with polarization is defined by the Equation (5) [12].

$$[\sigma] = \begin{bmatrix} \sigma_{HH} & \sigma_{HV} \\ \sigma_{VH} & \sigma_{VV} \end{bmatrix} \quad (5)$$

where σ_{uv} is uv -polarization components of radar cross section matrix defined by the Equation (6)

$$\sigma_{uv} = \lim_{R \rightarrow \infty} \left(4\pi R^2 \left| \frac{\vec{E}_{s,u}}{E_{i,v}} \right|^2 \right), \quad (u, v = H, V) \quad (6)$$

where R is the distance between the receiver and the center of the target, and $\vec{E}_{i,v}$ and $\vec{E}_{s,u}$ are the electric field vector of incident and scattered electromagnetic waves, respectively. And also the lower characters, H and V , represent the polarization of electromagnetic waves.

Assuming that the electromagnetic plane wave is incident to any target, the electric field vector scattered to a certain position \vec{E}_s satisfies the following Stratton-Chu integral equation [12]:

$$\vec{E}_s = -\frac{jk e^{-jkR}}{4\pi R} \int_S \left\{ \hat{\zeta}_s \times \left[\hat{n} \times \vec{E} - \tilde{z} \hat{\zeta}_s \times \left(\hat{n} \times \vec{H} \right) \right] \right\} e^{jk\vec{r} \cdot (\hat{\zeta}_s - \hat{\zeta}_i)} dS \quad (7)$$

where j is the unit imaginary ($= \sqrt{-1}$), S the target surface, k the wave number ($= \omega_0/c$), ω_0 the circular frequency, and c the speed of electromagnetic waves. $\hat{\zeta}_i$ and $\hat{\zeta}_s$ are the unit directional vectors of the incidence and scattering of the electromagnetic wave. \hat{n} is the unit normal vector at any position on the target surface. \vec{E} and \vec{H} are the electric field vector and the magnetic field vector induced on the surface, respectively. \vec{r} is the position vector of the receiver. \tilde{z} is the electromagnetic impedance of the medium (air).

As mentioned above, the physical optics is adopted for the last reflection point in the multiple scattering problem of the electromagnetic wave. Consider the flat surface of which the area is S and the local coordinates is defined as Fig. 3. By applying Kirchoff approximation, the Equation (7) can be rearranged by

$$\vec{E}_s = -\frac{jk e^{-jkR}}{2\pi R} E_0 \vec{W}(\hat{p}) \int_S e^{jk\vec{r} \cdot (\hat{\zeta}_s - \hat{\zeta}_i)} dS \quad (8)$$

where $E_0 (= |\vec{E}_i|)$ is the magnitude of the incident electromagnetic wave field vector \vec{E}_i . $\vec{W}(\hat{p})$ is the polarization vector with respect to the unit polarization vector $\hat{p} (= \vec{E}_i/E_0)$ and yields the following vector equation:

$$\begin{aligned} \vec{W}(\hat{p}) = & \frac{1}{2} \hat{\zeta}_s \times \left\{ (1 + \Gamma_E) (\hat{p} \cdot \hat{e}_\perp) (\hat{n} \times \hat{e}_\perp) + (1 - \Gamma_H) (\hat{p} \cdot \hat{e}_\parallel^i) (\hat{\zeta}_i \cdot \hat{n}) \hat{e}_\perp \right. \\ & + (1 - \Gamma_E) (\hat{p} \cdot \hat{e}_\perp) (\hat{\zeta}_i \cdot \hat{n}) (\hat{\zeta}_s \times \hat{e}_\perp) \\ & \left. - (1 + \Gamma_H) (\hat{p} \cdot \hat{e}_\parallel^i) \left[\hat{\zeta}_s \times (\hat{n} \times \hat{e}_\perp) \right] \right\} \end{aligned} \quad (9)$$

where Γ_E and Γ_H are the Fresnel reflection coefficients of an impedance (lossy) surface for E - and H -polarizations, respectively. \hat{e}_\perp and \hat{e}_\parallel^i are the vertical unit vector and the parallel unit vector with respect to the incident plane, respectively.

Meanwhile, the phase integral of the Equation (8) is calculated in the analytic form when the integral surface S is flat polygonal patches [13].

The geometric optics is adopted for the specular reflections not for the last reflection. In high-frequency range, the electromagnetic wave propagates straightly in a homogeneous medium as if it is a light, and the incident wave is reflected toward the specular direction by Snell's law, as shown in Fig. 4. The direction of the scattering $\hat{\zeta}_s$ is coincident with that of specular reflection $\hat{\zeta}_r$, and the polarization vector of the Equation (9) is simplified as

$$\vec{W}(\hat{p}) = - \left[\Gamma_E (\hat{p} \cdot \hat{e}_\perp) \hat{e}_\perp + \Gamma_H (\hat{p} \cdot \hat{e}_\parallel^i) \hat{e}_\parallel^s \right] (\hat{\zeta}_s \cdot \hat{n}) \quad (10)$$

where \hat{e}_\parallel^s is the parallel unit vector with respect to the incident plane defined in Fig. 4.

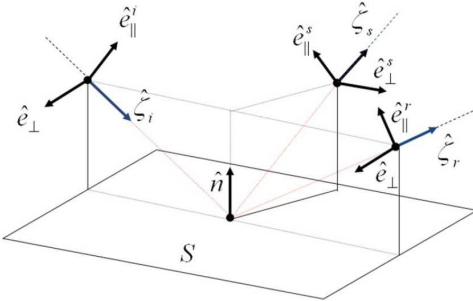


Figure 3. Local coordinates of an impedance surface.

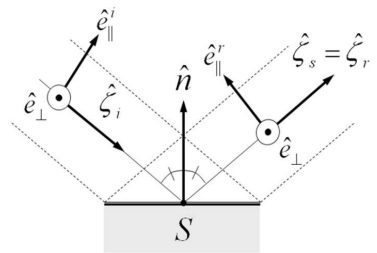


Figure 4. Specular reflection of the electromagnetic plane wave by a flat surface.

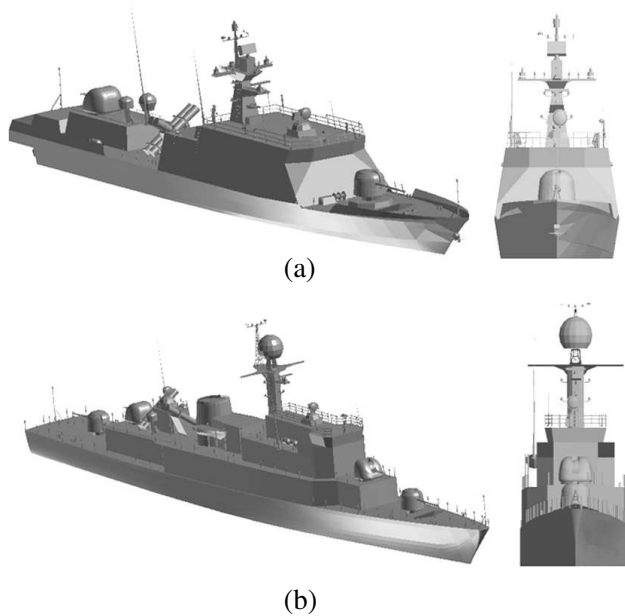


Figure 5. Isometric and front view of reference RCS model of the object naval ships; (a) Model-A and (b) Model-B.

The method introduced above requires a special process of extracting the hidden/visual surfaces and the multi-reflection surfaces to perform the phase integrals in the Equation (8). For this purpose, the hidden surface removal algorithm [13] is used in this paper.

3. NUMERICAL INVESTIGATION

3.1. Object Model and Analysis Condition

The dynamic RCS characteristics of two types of object ships have been numerically investigated. Model-A is a 63 m class stealthy naval ship, applying shaping techniques such as inclining hull and shielding outdoor equipment for RCS reduction, while Model-B is an 88 m class conventional (non-stealthy) naval ship, applying no RCS reduction techniques. Fig. 5 shows views of the reference RCS model of the object naval ships. Each model has been generated referring to the exterior drawings of the object naval ships above waterline. For reference, the reference RCS model of Model-A consists of 29,271 vertexes and 39,356

triangular facets and also that of Model-B of 29,007 vertexes and 24,829 triangular facets.

Table 1 shows the analysis conditions used for the ship motion calculation and the RCS analysis, where the incident angle of the radar wave and the ocean wave are defined as shown in Fig. 6.

Table 1. Conditions for the ship motion analysis and dynamic RCS analysis.

Model Name		Model-A	Model-B
Ship motion analysis	Ocean wave spectrum	JONSWAP spectrum	
	Ship speed (m/s)	0 (drift condition)	
	Significant wave height (m)	0.88/3.25	0.88
	Wave peak period (sec)	7.5/9.7	7.5
	Wave incident angle w.r.t forward direction (degrees)	0, 45, 90	45
Dynamic RCS analysis	Radar frequency (GHz)	10	
	Polarization	VV, HH	
	Incident angle (degrees)	Azimuth	0, 45, 90, 135, 180
Elevation		0	
time (sec)	Start	100	
	Finish	130	
	Step	0.02	

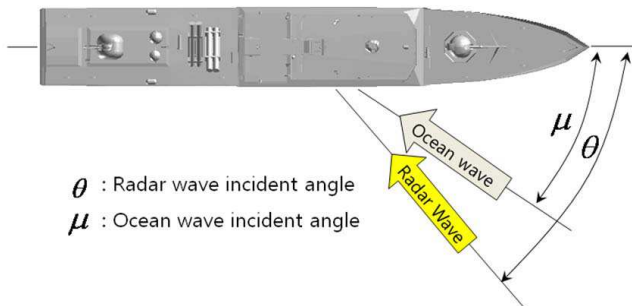


Figure 6. Definition of the incident angle of the radar wave and the ocean wave in a top view of the object naval ship.

3.2. Static RCS

For comparison with the dynamic RCS results hereafter, the RCS analyses have been carried out for both reference RCS model, i.e., static RCS, where the elevation angle is fixed to 0 degree and the azimuth angle changes from 0 to 360 degrees in 0.2 degree step. Fig. 7 represents the static RCS of Model-A and Model-B with respect to the radar wave incident angle (azimuth angle), respectively. On a whole, there is a little difference in pattern due to the exterior shape of the object ship, and also much fluctuation occurs in both results with respect to the azimuth angle. This means the RCS of the object naval ships could be highly depending on the ship's relative attitude to the radar wave incident direction. For reference, RCS values could not be indicated because of military security problems, instead of that, the RCS difference between tick marks has been expressed on the graphs.

3.3. Ship Motion Response

The transfer functions of the object naval ships have been calculated using a program based on a strip theory, MOTNHW [9].

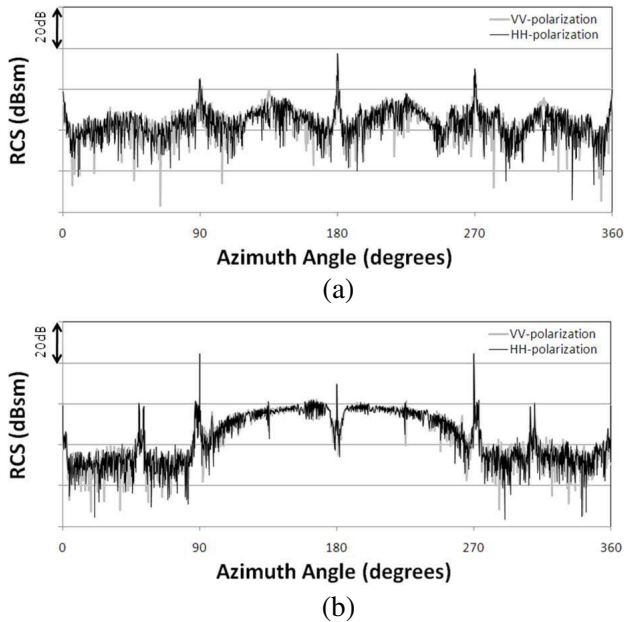


Figure 7. Static RCS analysis results; (a) Model-A and (b) Model-B.

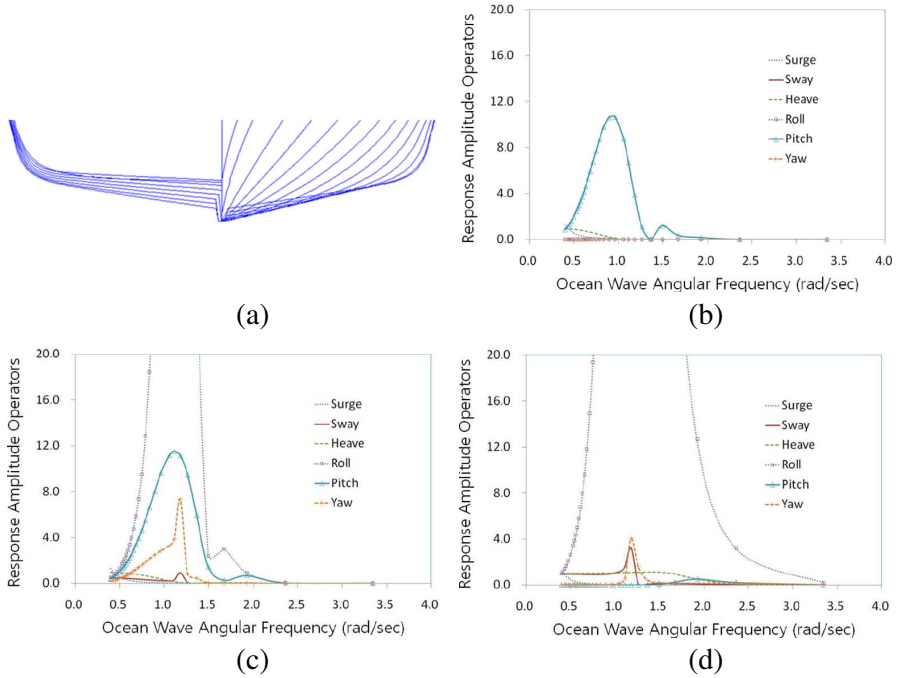


Figure 8. Ship motion analysis model and RAO of Model-A; (a) strip sections, (b) RAO ($\mu = 0$ degree), (c) RAO ($\mu = 45$ degrees), (d) RAO ($\mu = 9$ degrees).

Representatively, Fig. 8 shows the strip section and the RAOs of the Model-A. The ship motion characteristics are different against the ocean wave incident angle, as expected. Particularly, the pitch response is dominant for the ocean wave 0 degree of incident angle μ , while the roll response dominant for 45 and 90 degrees. The results have been used as the transfer functions for the time domain ship motion calculation with the Equation (1).

3.4. Dynamic RCS

Numerical calculations have been carried out for all cases mentioned in Table 1. For discussion, however, only two dynamic RCS analysis results of Model-A are representatively presented in Fig. 9 and Fig. 10, where the significant wave height and incident angle of ocean wave are 0.88 m and 45 degrees, respectively, but the incident angles of the radar wave are differently set to 45 and 135 degrees for Fig. 9 and Fig. 10, respectively. For intuitive comparison, the time-domain ship motion response for 6-DOF and the RCS value occurrence histograms

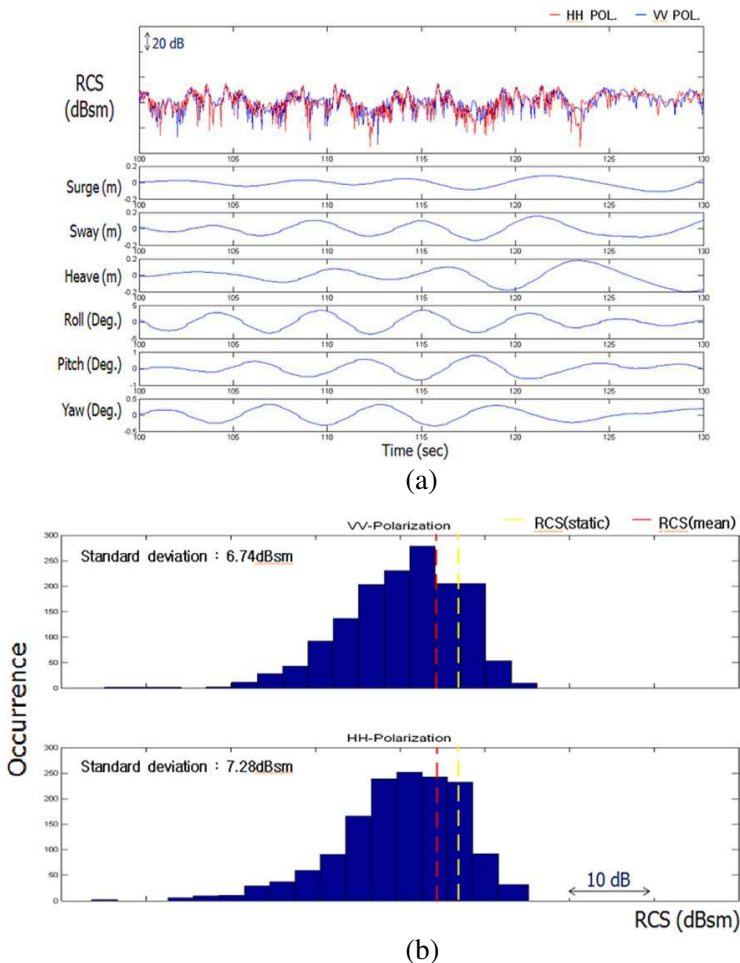


Figure 9. Dynamic RCS analysis result of Model-A (significant wave height = 0.88 m, $\theta = 45$ degrees, $\mu = 45$ degrees); (a) dynamic RCS and ship motion response in 6-DOF and (b) RCS occurrence histogram.

are indicated together.

The dynamic RCS considerably changes in time due to the ship motion, and the RCS values are lower than that of static RCS value (no ship motion) on a whole. Particularly, for the radar wave 45 degrees of incident angle, the mean RCS values are 3.45 and 3.31 dBsm lower, compared to those of static RCS value, for vertical and horizontal polarizations, respectively, where the standard deviations are 6.74 and

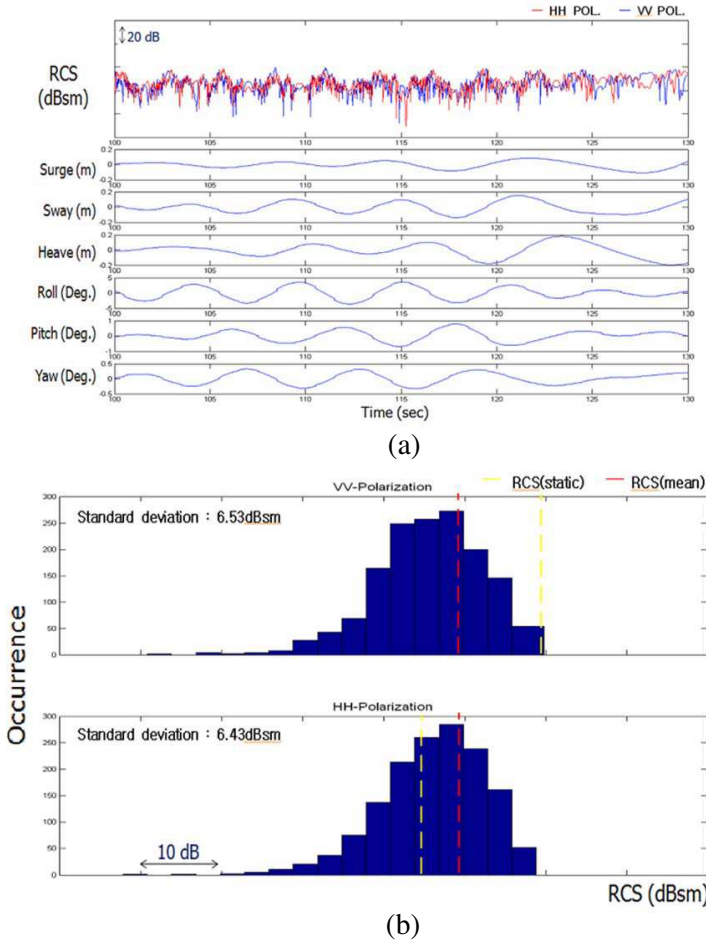


Figure 10. Dynamic RCS analysis result of Model-A (significant wave height = 0.88 m, $\theta = 135$ degrees, $\mu = 45$ degrees); (a) dynamic RCS and ship motion response in 6-DOF and (b) RCS occurrence histogram.

7.28 dBsm for vertical and horizontal polarizations, respectively. On the other hand, for 135 degrees of the radar wave incident angle, the mean RCS values are 10.5 dBsm lower and 5.2 dBsm higher, compared with those of static RCS value, for vertical and horizontal polarizations, respectively, where the standard deviations are 6.53 and 6.43 dBsm for vertical and horizontal polarizations, respectively.

In order to investigate the results more quantitatively, the relative mean RCS values to the static RCS values are summarized in Table 2

Table 2. Relative mean RCS values to the static RCS values in dBsm.

Model name	Sig. wave height (m)	Polarization	ocean wave		Incident angle of radar wave (deg.)				
			Inc. angle (deg.)		0	45	90	135	180
Model-A	0.88	VV	0		-0.5	-0.4	-0.1	-4.3	-1.8
			45		-0.9	-3.5	-5.2	-10.5	-9.6
			90		1.5	-4.7	-4.5	-12.5	-4.8
			Mean					-4.1	
		HH	0		-0.4	-0.3	-0.1	11.3	-1.8
			45		-0.9	-3.3	-4.5	5.2	-9.6
			90		0.9	-4.3	-3.6	3.2	-4.7
			Mean					-0.9	
	Mean						-2.5		
	3.25	VV	0		-3.7	-3.6	-0.1	-7.8	-6.9
			45		-8.5	-3.8	-9.7	-12.4	-17.1
			90		1.0	-3.8	-2.8	-11.3	-7.2
			Mean					-6.5	
		HH	0		-3.5	-3.5	-0.2	7.2	-6.9
45				-8.4	-3.6	-9.0	3.1	-17.2	
90				0.7	-3.7	-2.0	4.9	-7.0	
Mean							-3.3		
Mean						-4.9			
Model-B	0.88	VV	45	-11.2	0.4	-27.6	-4.6	-15.7	
		HH	45	-11.1	3.7	-27.6	-18.8	-15.7	
		Mean						-12.8	

with respect to the type of ship and the cases mentioned in Table 1, where the relative mean RCS values have been obtained by subtracting the dynamic RCS mean value from the static RCS value of the corresponding radar wave incident angle. The dynamic RCS of naval ship is affected considerably according to the type of the object ship, significant wave height and incident angle of ocean wave, and incident angle of radar wave. On a whole, the mean RCS is deviated from -17.19 to 11.26 dBsm for Model-A, and from -27.64 to 3.68 dBsm for Model-B, compared to the static RCS. In the mean RCS values of all conditions, it is shown that the non-stealthy ship, Model-B, is more affected by ship motion compared to the stealthy ship, Model-A. Particularly, as the significant wave is higher, the dynamic RCS values decrease, and also the RCS variations is rather less for *HH*-polarization than *VV*-polarization.

Meanwhile, in order to observe the major ship motion component affecting the dynamic RCS, additional calculations have been performed, in which the individual ship motion components have been considered as the ship motion data. The results have shown that the rotational components such as roll, pitch and yaw affect the dynamic

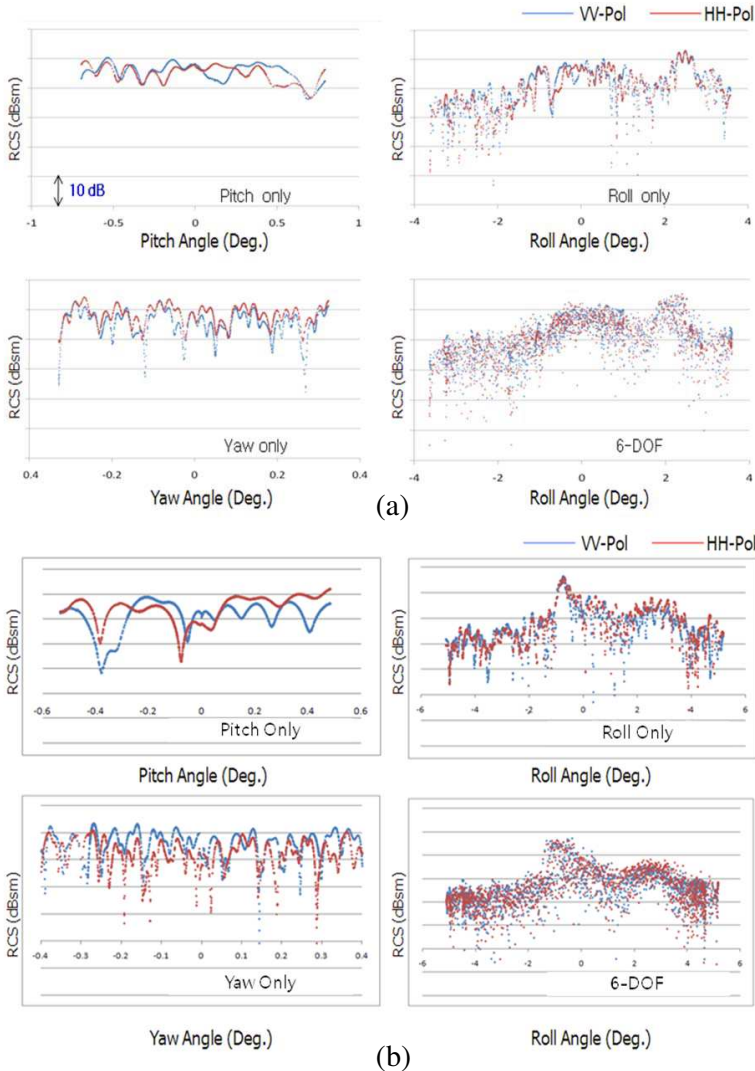


Figure 11. Correlations between RCS data when considering 1-DOF and 6-DOF ship response (significant wave height = 0.88 m, $\theta = 45$ degrees, $\mu = 45$ degrees); (a) Model-A and (b) Model-B.

RCS of the object ships, while the transitional components such as surge, sway and heave do not (independent of time). Fig. 11 represents the results for Model-A and Model-B as scatter plots when only considering the individual rotational ship motion component; pitch, roll and yaw, where the significant wave height is 0.88 m, the radar wave incident angle is 45 degrees, and the ocean wave incident angle is 45 degrees. By comparing the results with that of the consideration of all ship motion components, it is presumable that the roll component would be most correlated to the dynamic RCS, which is considered because the roll motion is the largest for the corresponding case as shown in Fig. 8(c).

4. CONCLUSION

In this study, the dynamic RCS characteristics of the naval ship have been numerically investigated for two types of naval ship using a quasi-static approach. From the results, it is observed that the RCS considerably changes in time due to the ocean wave-induced ship motion. On a whole, the dynamic RCS values are lower than the static RCS value (no ship motion) except for some cases. The dynamic RCS of naval ship is considerably affected due to type of the object ship, significant wave height, incident angle of ocean wave and radar wave and so on. Generally, the non-stealthy ship is rather more affected by ship motion than the stealthy ship. Particularly, as the significant wave is higher, the mean dynamic RCS values decrease. Also the RCS variations is rather less for *HH*-polarization than *VV*-polarization. The major component affecting the dynamic RCS is the roll motion.

Meanwhile, dynamic RCS is influenced by not only ocean wave-induced motion considered in this study but also the multi-path effect by interaction of ocean surface to ship hull. Therefore, a further study on their combined effects has to be required.

ACKNOWLEDGMENT

This work was supported by Republic of Korea Navy (ROKN) and the National Research Foundation of Korea (NRF) grant funded by the Korea government (MEST) through GCRC-SOP (Grant No. 2011-0030669 and No. 2011-0030686).

REFERENCES

1. Upson, C., I. McKenna, and K. Figg, "Test plan for full-scale radar signature measurements," BAE Systems,

- YD1484/RCS/TR.B10/v1, 2001.
2. Tice, T. E., "An overview of radar cross section measurement," *IEEE Transaction on Instrumentation and Measurement*, Vol. 39, No. 1, 205–207, 1990.
 3. Ojeda, J. F., J. L. Rodríguez, I. García-Tuñón, and F. Obelleiro, "Experimental verification of the relation between the radar cross section and the list angle of surface vessels," *Microwave and Optical Technology Letters*, Vol. 48, No. 11, 2237–2241, 2006.
 4. Jamil, K. and R. J. Burkholder, "Radar scattering from a rolling target floating on a time-evolving rough sea surface," *IEEE Transaction on Geoscience and Remote Sensing*, Vol. 44, No. 11, 3330–3337, 2006.
 5. Kim, K., J. H. Kim, T. M. Choi, Y. H. Kim, and D. S. Cho, "A study on a dynamic radar cross section analysis technique for a surface warship," *Journal of Ocean Engineering and Technology*, Vol. 23, No. 6, 77–81, 2009.
 6. Kim, K., D. S. Cho, and J. H. Kim, "High-frequency back-scattering cross section analysis of rotating targets," *Journal of the Korea Institute of Military Science and Technology*, Vol. 10, No. 3, 16–24, 2007.
 7. Lewis, E. V., *Principles of Naval Architecture (Vol. III): Motions in Waves and Controllability*, 3rd Edition, Society of Naval Architects and Marine Engineers, New York, 1988.
 8. MOERI, "User's guide of ship seakeeping analysis program (MOTNHW)," Ver. 2.0, KORDI, 2002.
 9. Kim, K., J. H. Kim, T. M. Choi, and D. S. Cho, "Development of radar cross section analysis system of complex marine targets," *International Journal of Naval Architecture and Ocean Engineering*, Vol. 4, No. 1, 20–32, 2012.
 10. Pérez, T. and M. Blanke, "Simulation of ship motion in seaway," Technical Report EE2037, University of Newcastle, 2002.
 11. Kim, K., J. H. Kim, and D. S. Cho, "Radar cross section analysis of marine targets using a combining method of physical optics/geometric optics and a Monte-Carlo simulation," *Ocean Engineering*, Vol. 36, No. 11, 821–830, 2009.
 12. Knott, E. F., M. T. Tuley, and J. F. Shaeffer, *Radar Cross Section*, 2nd Edition, Artech House Publisher, 1993.
 13. Kim, K., J. H. Kim, and D. S. Cho, "RCS analysis of complex structures using object precision method," *Journal of the Society of Naval Architects of Korea*, Vol. 42, No. 2, 159–164, 2005.